Received: 6 December 2020 | Accepted: 6 June 2021

DOI: 10.1111/2041-210X.13665

RESEARCH ARTICLE

Methods in Ecology and Evolution BRITISH ECOLOGICAL SOCIETY

A unifying framework for quantifying and comparing n-dimensional hypervolumes

Muyang Lu[1,2] | Kevin Winner[1,2] | Walter Jetz[1,2]

[1]Ecology and Evolutionary Biology, Yale University, New Haven, CT, USA

[2]Center for Biodiversity and Global Change, Yale University, New Haven, CT, USA

Correspondence
Muyang Lu
Email: muyang.lu@yale.edu

Funding information
National Science Foundation, Grant/Award Number: DEB-1441737; National Aeronautics and Space Administration, U.S.A., Grant/Award Number: 80NSSC17K0282 and 80NSSC18K0435

Handling Editor: Will Pearse

Abstract

1. The quantification of Hutchinson's n-dimensional hypervolume has enabled substantial progress in community ecology, species niche analysis and beyond. However, most existing methods do not support a partitioning of the different components of hypervolume. Such a partitioning is crucial to address the 'curse of dimensionality' in hypervolume measures and interpret the metrics on the original niche axes instead of principal components. Here, we propose the use of multivariate normal distributions for the comparison of niche hypervolumes and introduce this as the multivariate-normal hypervolume (MVNH) framework (R package available on https://github.com/lvmuyang/MVNH).
2. The framework provides parametric measures of the size and dissimilarity of niche hypervolumes, each of which can be partitioned into biologically interpretable components. Specifically, the determinant of the covariance matrix (i.e. the generalized variance) of a MVNH is a measure of total niche size, which can be partitioned into univariate niche variance components and a correlation component (a measure of dimensionality, i.e. the effective number of independent niche axes standardized by the number of dimensions). The Bhattacharyya distance (BD; a function of the geometric mean of two probability distributions) between two MVNHs is a measure of niche dissimilarity. The BD partitions total dissimilarity into the components of Mahalanobis distance (standardized Euclidean distance with correlated variables) between hypervolume centroids and the determinant ratio which measures hypervolume size difference. The Mahalanobis distance and determinant ratio can be further partitioned into univariate divergences and a correlation component.
3. We use empirical examples of community- and species-level analysis to demonstrate the new insights provided by these metrics. We show that the newly proposed framework enables us to quantify the relative contributions of different hypervolume components and to connect these analyses to the ecological drivers of functional diversity and environmental niche variation.
4. Our approach overcomes several operational and computational limitations of popular nonparametric methods and provides a partitioning framework that has wide implications for understanding functional diversity, niche evolution, niche shifts and expansion during biotic invasions, etc.

KEYWORDS
beta diversity, Bhattacharyya distance, entropy, environmental niche, functional diversity, generalized variance, hypervolume, standardized ellipse area

1 | INTRODUCTION

The n-dimensional hypervolume is one of the most fundamental (Holt, 2009; Hutchinson, 1957; Pulliam, 2000; Whittaker et al., 1973) and commonly used concepts (Blonder, 2018; Díaz et al., 2015; Pironon et al., 2018) in ecology and evolutionary biology. Hutchinson first proposed to describe species' niche as an n-dimensional hypervolume in which a species can survive and reproduce (Hutchinson, 1957). The use of hypervolume was later extended to describe functional space and trait space (Lamanna et al., 2014; Laughlin, 2014; Pigot et al., 2020). The geometric features of n-dimensional hypervolumes (especially their size and dissimilarity) are associated with a wide range of hypotheses and applications in ecology and evolution. For example, the size of a climatic niche hypervolume is hypothesized to drive species diversification rates: in mammals, species with narrower niches (specialists) have been shown to have higher speciation rates and lower extinction rates than those with wider niches (generalists) (Gómez-Rodríguez et al., 2015; Rolland & Salamin, 2016). The size of climatic niche hypervolume is also hypothesized to drive the variation of geographical range size (Cardillo et al., 2019; Ficetola et al., 2020; Saupe et al., 2015; Slatyer et al., 2013). Similarity between species' environmental niche hypervolumes or functional trait hypervolumes is used to measure niche divergence or niche packing, which is hypothesized to determine species' coexistence and species richness patterns (Castro-Insua et al., 2018; Kuppler et al., 2017; Pigot et al., 2016; Read et al., 2018; Serra-Varela et al., 2015). Niche similarity is also used for within-species comparisons such as assessing the impact of climate change (Gómez et al., 2016; Tayleur et al., 2015; Zurell et al., 2018) and whether there are niche shifts during biotic invasions (Carvalho & Cardoso, 2020; Davies et al., 2019; Early & Sax, 2014; Guisan et al., 2014; Lauzeral et al., 2011).

The quantification of niche volume and similarity has thus become an urgent pursuit for both theoretical investigation and real-world applications. Recently, nonparametric methods, such as kernel-density estimates (Blonder et al., 2014, 2018; Carvalho & Cardoso, 2020; Eckrich et al., 2020; Mammola & Cardoso, 2020), dynamic range boxes (Junker et al., 2016), minimum convex hulls (Blonder et al., 2018), support vector machines (Blonder et al., 2018; Brown et al., 2020) and α-shapes (Gruson, 2020), have been widely favoured because of their minimal assumptions around the distribution of data and the existence of well-documented statistical packages supporting their exploration and use. In most of these methods, an n-dimensional distribution over environmental or trait space is typically converted to a hypervolume with a boundary defined by a particular quantile (often 95%) of the distribution. Niche size is calculated as the volume of the enclosed space. Niche similarity of two hypervolumes can then be quantified in multiple ways, either with the union and intersection of hypervolumes (Jaccard and Sorensen indices) or with the distances between the two hypervolumes (Loiseau et al., 2017; Mammola, 2019).

These nonparametric methods of quantifying hypervolumes have several methodological limitations: (a) niche volumes and similarity measures are sensitive to the parameterization of the underlying distribution (e.g. choice of bandwidth in KDE) and depend additionally on the choice of quantile (e.g. 95%) except for the dynamic range box (Junker et al., 2016); (b) computational costs are high when the dimension of variables and sample size are large (Blonder et al., 2014) and most importantly (c) the nonparametric methods generally cannot say anything about the relative importance of the constituent components of the measures (but see Junker et al., 2016; Loiseau et al., 2017). For those that do enable a partitioning (e.g. dynamic range box; Junker et al., 2016), they do not measure the contribution of correlations among niche axes to total hypervolume variations. Moreover, the lack of partitioning framework along niche axes also makes nonparametric methods more sensitive to the number of dimensions, as the number of observations required to accurately estimate an empirical distribution increases exponentially with the number of dimensions, hence the 'curse of dimensionality' (Blonder, 2016).

The prevalence of nonparametric methods in quantifying hypervolumes also hampers the integration of empirical niche studies with niche theories because empirical metrics are disconnected from theoretical derivations. For example, in the theory of limiting similarity, the outcomes of competition exclusion and niche evolution are typically calculated from one-dimensional utilization curves (Leimar et al., 2013; MacArthur & Levins, 1967). However, the testable theoretical predictions derived by these studies rely on empirical analyses in higher dimensions (Rappoldt & Hogeweg, 1980), meaning that with the prevalent nonparametric methods, hypotheses such as 'higher niche similarity causes more competitive exclusion' cannot be directly tested against analytical predictions derived from theories (D'Andrea & Ostling, 2016; Kuppler et al., 2017). Although various parametric dissimilarity metrics have been proposed (Morisita, 1961; Pianka, 1974; Lu et al., 1989), they were largely overlooked because of their conceptual disconnection with the prevalent size metrics of hypervolume. Parametric measures that have clear analytical links to theories are urgently needed.

To fill in this gap, we propose a framework to quantify and partition niche volume and dissimilarity based on the assumption of multivariate normal (MVN) distribution of the variables under study and call this the multivariate normal hypervolume (MVNH) framework. This partitioning framework provides a powerful quantitative assessment of the relative contributions of the constituent components in driving total niche variation. We chose the multivariate normal distribution because it is the most widely used assumption for niche assessment and modelling both in theoretical (Jiménez et al., 2019; MacArthur & Levins, 1967;

Rappoldt & Hogeweg, 1980; Soberón & Nakamura, 2009) and empirical work (González et al., 2017; La Sorte et al., 2018), which provides room for integration and synthesis of size and dissimilarity measures (Lu et al., 1989). We show that in the MVNH framework niche size can be derived from the covariance matrix (Soberón & Nakamura, 2009), and that niche dissimilarity can be quantified by the Bhattacharyya distance (Bhattacharyya, 1946; Lu et al., 1989; Winner et al., 2018). We demonstrate theoretically and with empirical examples how the partitioning of the metrics reveals the key drivers of variation in functional diversity and environmental niche.

2 | MATERIALS AND METHODS

In our MVNH framework, we propose that a multi-dimensional niche space be described by a multivariate normal distribution with probability density function:

$$f_x(x) = \frac{\exp\left(-\frac{1}{2}(\mathbf{x}-\boldsymbol{\mu})^T\Sigma^{-1}(\mathbf{x}-\boldsymbol{\mu})\right)}{\sqrt{(2\pi)^n\,|\Sigma|}}, \quad (1)$$

where $x = \{x_1, \ldots, x_n\}$ is a vector in the n-dimensional niche space, $\mu = \{\mu_1, \ldots, \mu_n\}$ is the centroid, Σ is the covariance matrix for the n-dimensional niche and $|\Sigma|$ denotes the determinant of the covariance matrix.

2.1 | The size of a hypervolume

We define the size of a hypervolume as the determinant of the covariance matrix $|\Sigma|$, also called the 'generalized variance' (La Sorte et al., 2018). It has a geometric interpretation as the volume of the n-dimensional parallelepiped spanned by the column or row vectors of the covariance matrix. For example, the covariance matrix Σ and the generalized variance $|\Sigma|$ of a two-dimensional MVNH are:

$$\sum = \begin{bmatrix} \sigma_x^2 & \rho_{xy}\sigma_x\sigma_y \\ \rho_{xy}\sigma_x\sigma_y & \sigma_y^2 \end{bmatrix}, \quad (2)$$

$$\left|\sum\right| = \sigma_x^2\sigma_y^2\left(1-\rho_{xy}^2\right), \quad (3)$$

where σ_x^2 is the variance of variable x, σ_y^2 is the variance of variable y and ρ_{xy} is the correlation coefficient between the two environmental variables x and y. When log-transformed, Equation 3 enables us to additively partition the size of a two-dimensional hypervolume into three separate components (Figure 1c; also see empirical examples of functional diversity and environmental niche breadth): the variance of the first niche axis σ_x^2, the variance of the second niche axis σ_y^2 and a correlation component $(1 - \rho_{xy}^2)$. The correlation component can be seen as a shrinkage factor which shrinks the niche volume by a factor of $(1 - \rho_{xy}^2)$. The correlation component can also be calculated as the determinant of the correlation matrix, which is a measure of hypervolume dimensionality (i.e. the effective number of independent niche axes standardized by the number of dimensions) in itself.

Similarly, for a three-dimensional hypervolume, the determinant of the covariance matrix is:

$$|\Sigma| = \sigma_x^2\sigma_y^2\sigma_z^2\left(1-\rho_{xy}^2-\rho_{yz}^2-\rho_{xz}^2+2\rho_{xy}\rho_{yz}\rho_{xz}\right), \quad (4)$$

where $\left(1-\rho_{xy}^2-\rho_{yz}^2-\rho_{xz}^2+2\rho_{xy}\rho_{yz}\rho_{xz}\right)$ is the correlation component. The factoring of the determinant generalizes straightforwardly to higher dimensions: the determinant is just the product of all univariate variances and a correlation component.

The determinant also has a close relationship with the standardized ellipse area (SEA, the ellipse with its major and minor axes defined by the principal components; Jackson et al., 2011): it scales with the SEA by a constant (π for a two-dimensional niche and $4\pi/3$ for a three-dimensional niche) and is therefore unaffected by rotation operations such as PCA. Factoring the determinant (as in Equations 3 and 4) can be used to assess the relative importance of the separate components in driving hypervolume size variations, such as when assessing whether individual trait axes or the constraint on the combination of traits (Dwyer & Laughlin, 2017) is the stronger driver of community functional diversity (see the empirical example of functional diversity).

2.2 | The dissimilarity of hypervolumes

We suggest measuring the dissimilarity of two hypervolumes with the Bhattacharyya distance (Bhattacharyya, 1946; Lu et al., 1989; Minami & Shimizu, 1999; Fieberg & Kochanny, 2005; Winner et al., 2018). The Bhattacharyya distance (BD) of two continuous probability distributions, A and B defined on the same domain $\mathcal{X}$ is:

$$\mathrm{BD}(A,B) = -\log \mathrm{BC}(A,B), \quad (5)$$

where BC is the Bhattacharyya coefficient:

$$\mathrm{BC}(A,B) = \int_{x\in\mathcal{X}} \sqrt{A(x)B(x)}\,\mathrm{d}x. \quad (6)$$

Therefore, for two probability distributions, the BC ranges from 0 to 1 and the BD thus ranges from 0 to ∞.

For two multivariate normal hypervolumes A and B, the BD has a closed form:

$$\mathrm{BD}(A,B) = \underbrace{\frac{1}{8}\left(\boldsymbol{\mu}_A-\boldsymbol{\mu}_B\right)^T\overline{\Sigma}^{-1}\left(\boldsymbol{\mu}_A-\boldsymbol{\mu}_B\right)}_{\mathrm{MD}} + \underbrace{\frac{1}{2}\ln\left(\frac{|\overline{\Sigma}|}{\sqrt{|\boldsymbol{\Sigma}_A|\,|\boldsymbol{\Sigma}_B|}}\right)}_{\mathrm{DR}}, \quad (7)$$

where $\boldsymbol{\mu}_A$ and $\boldsymbol{\mu}_B$ are the centroids of A and B, respectively, and $\overline{\Sigma}$ is the mean of the covariance matrices of A and B:

$$\overline{\Sigma} = \frac{\Sigma_A+\Sigma_B}{2}, \quad (8)$$

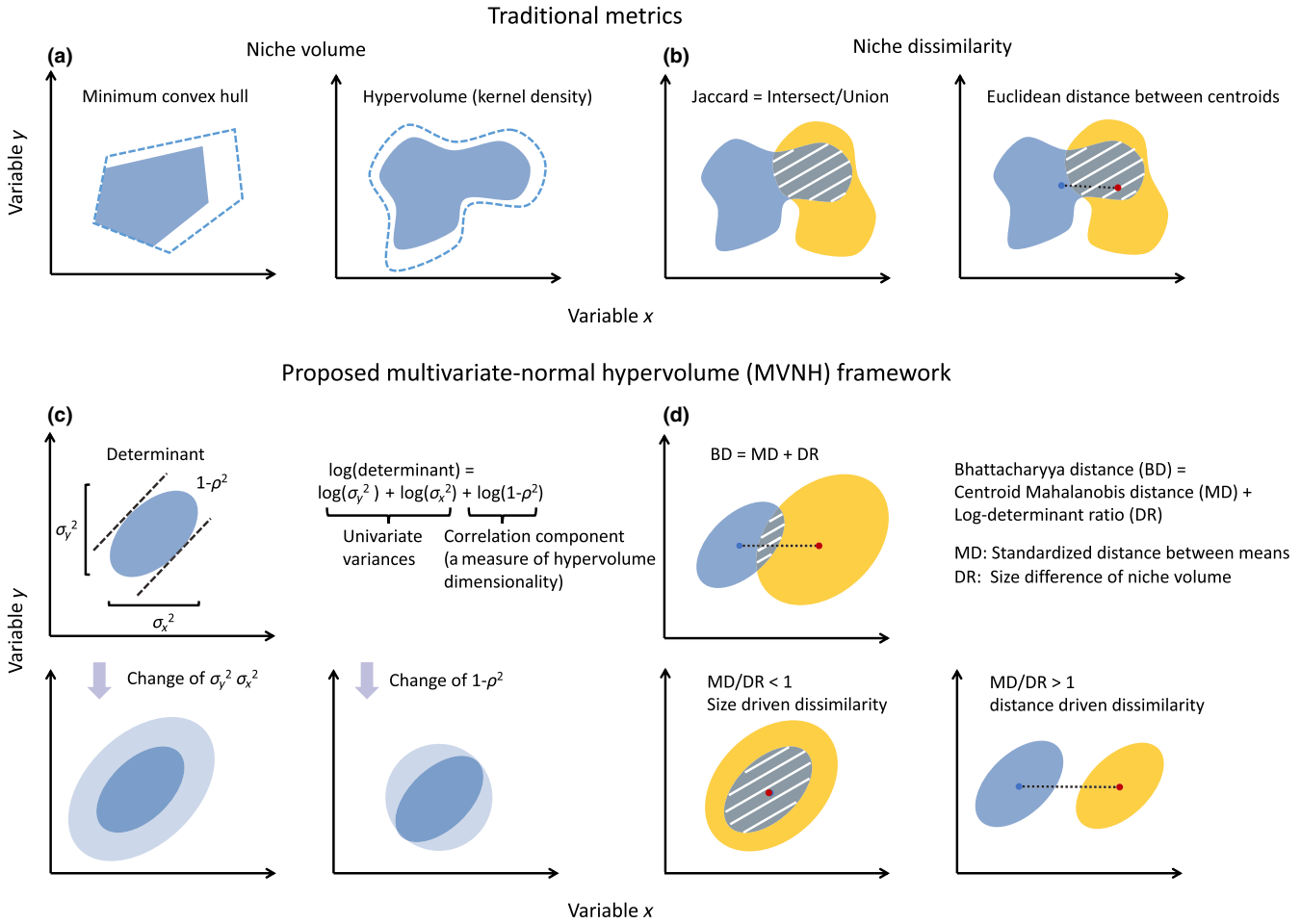

FIGURE 1 (a) Two commonly used nonparametric niche volume measures: the minimum convex hull and the kernel density estimated hypervolume. The filled area indicates the 95% contour of the hypervolume while the dashed blue lines indicate the 90% contour of the hypervolumes. (b) Two commonly used dissimilarity measures based on nonparametric volume estimates: Jaccard similarity and Euclidean distance between centroids. Orange and blue represent two hypervolumes. White hatches indicate intersecting area between two hypervolumes. (c) The volume of the two-dimensional niche measured by the determinant of the covariance matrix is the product of three components: two univariate variances (σ_x^2 and σ_y^2) and a correlation component (a measure of hypervolume dimensionality, i.e. the effective number of independent niche axes standardized by the number of dimensions) which has the effect of shrinking the volume by a factor of $(1-\rho^2)$. Light blue indicates change of hypervolume. (d) Niche dissimilarity of two hypervolumes measured by the Bhattacharyya distance, which is the sum of the Mahalanobis distance between the two niche centroids and a determinant ratio component measuring the difference of the niche volumes. The ratio MD/DR indicates the relative importance of centroid distance and size difference

The first term in Equation 7 is the Mahalanobis distance (MD) between two hypervolume centroids, and the second term in Equation 7 is the determinant ratio (DR) which measures the size difference between A and B (see Figure 1d). If two hypervolumes have the same size, then the second term in Equation 7 equals 0. Factoring the Bhattacharyya distance according to Equation 7 can be used to assess the relative contributions of the centroid difference (MD) and the size difference (DR) to the overall niche dissimilarity. The ratio of Mahalanobis distance to determinant ratio (MD/DR) can be used as an overall measure of the relative importance of centroid distance and size difference in driving overall dissimilarity.

The Mahalanobis distance component in Equations 7 can be linked to an existing partitioning framework which additively partitions the Mahalanobis distance into standardized Euclidean distances along PCA axes (Calenge et al., 2008; Mahony et al., 2017). But to align this approach with the framework developed here, we propose an alternative partitioning of the Mahalanobis distance into univariate divergence components and a correlation component, following a method from portfolio analysis in the finance literature to assess the risk-return trade-off of investments (Stevens, 1998). In the case of two-dimensional hypervolumes, the Mahalanobis distance can be written as:

$$\begin{aligned}\left(\boldsymbol{\mu}_A-\boldsymbol{\mu}_B\right)^T\overline{\Sigma}^{-1}\left(\boldsymbol{\mu}_A-\boldsymbol{\mu}_B\right)&=\frac{d_x^2}{\overline{\sigma}_x^2}+\frac{d_y^2}{\overline{\sigma}_y^2}\\&+\frac{1}{|\overline{\Sigma}|}\left(\overline{\rho}_{xy}^2\left(d_x\overline{\sigma}_x-d_y\overline{\sigma}_y\right)^2+2\overline{\rho}_{xy}d_xd_y\overline{\sigma}_x\overline{\sigma}_y\left(\overline{\rho}_{xy}-1\right)\right),\end{aligned}\tag{9}$$

where d_1 and d_2 are the Euclidean distances between niche centroids along variable 1 and variable 2, $\overline{\sigma}_x^2$,$\overline{\sigma}_y^2$ and $\overline{\rho}_{xy}$ are parameters of the mean covariance matrix $\overline{\Sigma}$. The first two terms are just the standardized

Euclidean distances along each dimension, and the last term is a correlation component which measures how much of the additional divergence (or convergence) is caused by the correlation between variables in the mean covariance matrix $\overline{\Sigma}$. The correlation component is negative when the direction of the centroid difference is close to the direction of the major principal component of $\overline{\Sigma}$, because it effectively decreases the standardized Euclidean distances between centroids. The correlation component is positive when the direction of the centroid difference is close to the direction of the minor principal component of $\overline{\Sigma}$, because it effectively increases the standardized Euclidean distances. Combining Equations (3), (7) and (9) and after some rearrangements of the terms, the Bhattacharyya distance in the two-dimensional case can be written as:

$$\begin{aligned} \mathrm{BD}(A,B) = {} & \frac{d_x^2}{8\overline{\sigma}_x^2} + \frac{1}{2}\ln\left(\frac{\overline{\sigma}_x^2}{\sqrt{\sigma_{xA}^2\sigma_{xB}^2}}\right) + \frac{d_y^2}{8\overline{\sigma}_y^2} + \frac{1}{2}\ln\left(\frac{\overline{\sigma}_y^2}{\sqrt{\sigma_{yA}^2\sigma_{yB}^2}}\right) \\ & + \frac{1}{8|\overline{\Sigma}|}\left(\overline{\rho}_{xy}^2\left(d_x\overline{\sigma}_x - d_y\overline{\sigma}_y\right)^2 + 2\overline{\rho}_{xy}d_xd_y\overline{\sigma}_x\overline{\sigma}_y\left(\overline{\rho}_{xy}-1\right)\right) + \frac{1}{2}\ln\left(\frac{1-\overline{\rho}_{xy}^2}{\sqrt{\left(1-\rho_{xyA}^2\right)\left(1-\rho_{xyB}^2\right)}}\right), \end{aligned} \tag{10}$$

which partitions the BD between two MVNHs into contributions of univariate components and a correlation component.

2.3 | Estimators

We used sample means and sample covariances as estimators of μ_A, μ_B, Σ_A and Σ_B for the calculation of the determinant of the covariance matrices and the Bhattacharyya distance. These plug-in estimators of the Bhattacharyya distance are known to be biased with small sample size, but for low-dimensional data this bias is small (Lu et al., 1989; Minami & Shimizu, 1999; Winner et al., 2018; also see Figures S2 and S3 in supplementary analysis). For the purpose of demonstrating the utility of the partitioning framework, our empirical analysis proceeds without applying bias-correction methods which have been presented in the literature such as estimating the covariance matrix using Bayesian methods (Swanson et al., 2015), and bias-correction techniques for the Bhattacharyya distance (Minami & Shimizu, 1999; Winner et al., 2018). Functions for calculating the size and dissimilarity metrics in the MVNH framework are available on GitHub in the package MVNH (Lu et al., 2021), which can be installed with R command devtools: install_github ('lvmuyang/MVNH'). We also include an example R script to demonstrate the use of the functions in supplementary materials (Appendix 2).

We also recognize other dissimilarity metrics (also included in the package) based on multivariate normal distributions which share a similar form with the Bhattacharyya distance and can be partitioned into a Mahalanobis distance component and a determinant ratio component (see Lu et al., 1989), such as the MacArthur–Levins measure (MacArthur & Levins, 1967):

$$\begin{aligned} \text{MacArthur - Levins}(A,B)_A &= \underbrace{\left(\boldsymbol{\mu}_A-\boldsymbol{\mu}_B\right)^T\overline{\boldsymbol{\Sigma}}^{-1}\left(\boldsymbol{\mu}_A-\boldsymbol{\mu}_B\right)}_{\mathrm{MD}} + \underbrace{\ln\left(\frac{|\overline{\boldsymbol{\Sigma}}|}{|\boldsymbol{\Sigma}_A|}\right)}_{\mathrm{DR}}, \\ \text{MacArthur - Levins}(A,B)_B &= \underbrace{\left(\boldsymbol{\mu}_A-\boldsymbol{\mu}_B\right)^T\overline{\boldsymbol{\Sigma}}^{-1}\left(\boldsymbol{\mu}_A-\boldsymbol{\mu}_B\right)}_{\mathrm{MD}} + \underbrace{\ln\left(\frac{|\overline{\boldsymbol{\Sigma}}|}{|\boldsymbol{\Sigma}_B|}\right)}_{\mathrm{DR}}, \end{aligned} \tag{11}$$

the Pianka's measure (Pianka, 1974):

$$\text{Pianka}(A,B)_A = \underbrace{\left(\boldsymbol{\mu}_A-\boldsymbol{\mu}_B\right)^T\overline{\boldsymbol{\Sigma}}^{-1}\left(\boldsymbol{\mu}_A-\boldsymbol{\mu}_B\right)}_{\mathrm{MD}} + \underbrace{\frac{1}{2}\ln\left(\frac{|\overline{\boldsymbol{\Sigma}}|}{\sqrt{|\boldsymbol{\Sigma}_A||\boldsymbol{\Sigma}_B|}}\right)}_{\mathrm{DR}}, \tag{12}$$

and the Morisita's measure (Morisita, 1961):

$$\text{Morisita}(A,B) = \underbrace{\left(\boldsymbol{\mu}_A-\boldsymbol{\mu}_B\right)^T\overline{\boldsymbol{\Sigma}}^{-1}\left(\boldsymbol{\mu}_A-\boldsymbol{\mu}_B\right)}_{\mathrm{MD}} + \underbrace{\ln\left(\frac{\sqrt{|\overline{\Sigma}|}\left(\sqrt{|\Sigma_A|}+\sqrt{|\Sigma_B|}\right)}{2\sqrt{|\Sigma_A||\Sigma_B|}}\right)}_{\mathrm{DR}}, \tag{13}$$

These metrics differ in their probabilistic interpretations, weighting of each component, and how they calculate the determinant ratio component. We will focus on the use of the Bhattacharyya distance in this paper because it was most studied and with known statistical properties (Lu et al., 1989; Minami & Shimizu, 1999; Winner et al., 2018). It also has a straightforward interpretation as the integration of geometric means of two probability distributions (Equation 6).

2.4 | Community example: Functional diversity and turnover

We used a trait dataset of 36 annual plant communities in the Western Australia (Data availabile from the Dryad Digital Repository https://doi.org/10.5061/dryad.76kt8; Dwyer & Laughlin, 2018) to demonstrate how functional diversity (alpha diversity) and turnover (beta diversity) can be measured in the multivariate normal hypervolume framework using the determinant and the Bhattacharyya distance, respectively. The three measured traits for each species were specific leaf area (SLA), maximum height (MH) and seed mass (SM). We then assessed each component of the trait volume (SLA variance, MH variance, SM variance and the correlation component)

as predicted by growing season available moisture, mean growing season minimum temperature and soil surface dispersion (dispersion is a measure of heterogeneity) in multiple linear regression. We used the coefficient of variation of each component to assess the relative contribution of each component to the variation of total trait volume because the individual niche variances are scalable and not directly comparable with each other. We assessed the environmental drivers of the Bhattacharyya distance (functional turnover) components using multiple regression on distance matrices (MRM) based on a partial Mantel test (Lichstein, 2007). The regression coefficients of MRM are calculated with ordinary least square regression, but the p-values of the coefficients are calculated with matrix permutation tests. The predictor variables were calculated as the Euclidean distances for each environmental variable between sites.

2.5 | Species example: Environmental niche breadth and dissimilarity

We studied 260 bird species in the Western hemisphere with occurrence data extracted from eBird (Sullivan et al., 2009), environmental layers obtained from CHELSA (monthly mean temperature and precipitations for breeding seasons, https://chelsa-climate.org/) and MODIS EVI (https://modis.gsfc.nasa.gov/data/dataprod/mod13.php) at 1 km resolution to assess the drivers of realized environmental niche breadth (volume) and niche dissimilarity between species. For each species, 1,000 random points were sampled and spatially thinned to 10 km distance using the spThin package (Aiello-Lammens et al., 2015) in R for extraction of environmental data. We then investigated the drivers of environmental niche breadth components using ordinary multiple linear regression, and assessed the drivers of the Bhattacharyya distance components using MRM. We obtained body mass and dietary niche breadth data from the 'EltonTrait' dataset (Wilman et al., 2014). Area and centroid absolute latitude of geographical range were calculated from IUCN range maps (https://www.iucnredlist.org/resources/spatial-data-download).

2.6 | Comparisons to nonparametric metrics

For both the community and species' niche examples, we compared the newly proposed size and dissimilarity metrics from the MVNH framework with measures based on the 95% quantile of a box kernel density estimator using the hypervolume package in R (Blonder et al., 2018). For the species environmental niche example, we also compared the determinant of the MVNH with the volume of minimum convex hull (Figure 1a); for the community functional diversity example, we additionally compared the determinant with three commonly used functional diversity measures: functional divergence, functional dispersion and functional evenness (Laliberté & Legendre, 2010). For both examples, we compared the Bhattacharyya distance with Jaccard and Sorensen similarities, centroid distances (Figure 1b) and minimum distances between hypervolumes. We then assessed the performance of our metrics with different sample size, number of dimensions and underlying distributions, and also compared them with other existing methods using simulated data (Appendix 1).

3 | RESULTS

We use the MVNH framework to first analyse drivers of community-level functional diversity and functional turnover, and to second assess drivers of species-level environmental niche breadth and dissimilarity. Finally, we show the correlations between the proposed metrics and other commonly used nonparametric measures.

3.1 | Community level: Functional diversity

We compared functional diversity (measured as the determinant of the trait covariance matrix) and functional turnover (measured as Bhattacharyya distance) among 36 plant communities. For a two-community example (site 1 and site 2), we partitioned the functional diversity of each site into four components: the univariate variance of each of the three traits (SLA, MH and SM) and the correlation component following Equation 4. Component-wise differences between the two sites add up to the difference in total trait volume (the determinant of the environmental niche covariance matrix) on the log-scale (Figure 2a).

For the 36-community assessment, the coefficient of variation for each trait volume component across the 36 sites was 0.31 for the correlation component and varied between 0.28 (MH) and 0.16 (SM) for the individual trait variances. This suggests that the correlation component is the largest driver of the variation in functional diversity among sites. By relating individual trait variances and the correlation component to environmental predictors, we identify mean moisture availability and, less so, minimum temperature as key correlates of trait diversity variation (Figure 2c,d). The variances of all three traits differ substantially in the strength and direction of their respective associations with environmental predictors. Linear regression shows that none of the examined environmental variables predict the variation of SLA variance (Table 1). Both minimum temperature and moisture availability are positively correlated with maximum height

FIGURE 2 Community-level functional diversity assessment. Component-wise differences between site 1 and site 2 in (a) functional trait volume (e.g. functional diversity) and (b) Bhattacharyya distance of functional traits. (c–f) Change of trait volume and pairwise community-level trait dissimilarity among all 36 sites of annual plant communities with environmental variables in southwest Western Australia. Solid lines are the fitted linear regression. Shaded area represents 95% confidence interval of linear regression. See Table 1 for summary statistics

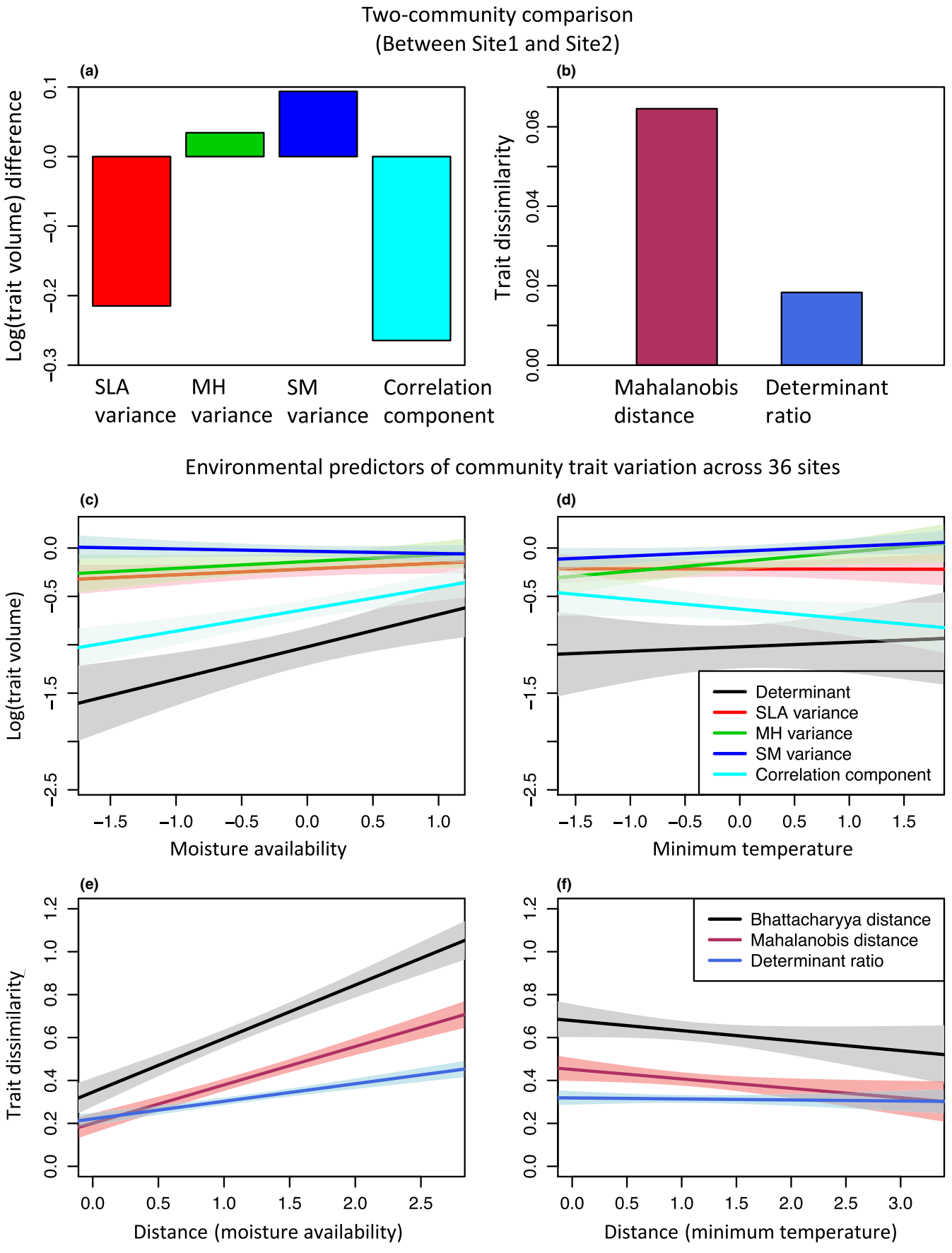
Two-community comparison
(Between Site1 and Site2)
(a)
Log(trait volume) difference
0.1
0.0
−0.1
−0.2
−0.3
SLA variance
MH variance
SM variance
Correlation component
(b)
Trait dissimilarity
0.06
0.04
0.02
0.00
Mahalanobis distance
Determinant ratio
Environmental predictors of community trait variation across 36 sites
(c)
Log(trait volume)
0.0
−0.5
−1.5
−2.5
−1.5
−1.0
−0.5
0.0
0.5
1.0
Moisture availability
(d)
0.0
−0.5
−1.5
−2.5
−1.5
−1.0
−0.5
0.0
0.5
1.0
1.5
Minimum temperature
Determinant
SLA variance
MH variance
SM variance
Correlation component
(e)
Trait dissimilarity
1.2
1.0
0.8
0.6
0.4
0.2
0.0
0.0
0.5
1.0
1.5
2.0
2.5
Distance (moisture availability)
(f)
1.2
1.0
0.8
0.6
0.4
0.2
0.0
0.0
0.5
1.0
1.5
2.0
2.5
3.0
Distance (minimum temperature)
Bhattacharyya distance
Mahalanobis distance
Determinant ratio

TABLE 1 Summary statistics for multiple linear regression of community-level trait volumes, and multiple regression on distance matrices on community-level trait dissimilarity. Specific leaf area, maximum height, seed mass variances, the correlation component and the determinant are log-transformed. Adjusted R^2 is used. Only significant predictors are reported

Response	Predictor	Estimate	*p*-value	R^2
Specific leaf area variance	—	—	—	—
Maximum height variance	Minimum temperature	0.125	<0.01	0.19
	Moisture availability	0.102	<0.05	
Seed mass variance	Soil surface dispersion	0.066	<0.05	0.25
Correlation component	Moisture availability	0.228	<0.001	0.37
Determinant	Moisture availability	0.369	<0.001	0.27
Mahalanobis distance	Distance (moisture availability)	0.18	<0.001	0.20
	Distance (minimum temperature)	−0.07	<0.05	
Determinant ratio	Distance (moisture availability)	0.08	<0.001	0.13
Bhattacharyya distance	Distance (moisture availability)	0.26	<0.001	0.18

variance, whereas only soil surface dispersion is positively correlated with seed mass variance. Moisture availability is also positively correlated with the correlation component. The overall trait volume (the determinant) is only correlated with moisture availability (Table 1).

We measured the pairwise functional turnover between any two sites as the Bhattacharyya distance between their hypervolumes, and, according to Equation 7, partitioned it into the Mahalanobis distance (which measures the standardized distance between community means) and the determinant ratio (which measures the differences in functional alpha diversity) (see a two-community example in Figure 2b). The ratio of Mahalanobis distance to determinant ratio (MD/DR) reflects the relative importance of difference in community means and functional diversity differences in driving the overall community-level functional turnover. The median ratio MD/DR across all pairs of sites is 0.63, suggesting functional turnover among communities is mainly driven by the variation in functional alpha diversity. The functional turnover is more determined by moisture availability than by minimum temperature (Figure 2e,f). Multiple regression on distance matrices suggests that the Mahalanobis distance is correlated with both minimum temperature and moisture availability, but the determinant ratio is only correlated with moisture availability (Table 1).

3.2 | Species level: Environmental niches

We used the presented method to analyse and compare the three-dimensional environmental niches (temperature, precipitation and EVI) of 260 bird species in the New World. We partitioned the total environmental niche volume for each single species into three univariate components and a correlation component. For a two-species example, we attributed the difference in niche volume between the white-throated swift *Aeronautes saxatalis* and the tricolored blackbird *Agelaius tricolor* to differences in temperature variance, precipitation variance, EVI variance and the correlation component (Figure 3a). For the 260-species assessment, we found that the coefficient of variation for each of the niche volume components among 260 bird species was 0.79 for precipitation variance, 0.67 for temperature variance, 0.44 for EVI variance and 0.22 for the correlation component, suggesting that precipitation niche breadth variation contributes most to the species-level niche volume variation. Range size and centroid latitude are the two main drivers of realized environmental niche volume (Figure 3c,d), but the predictors for each niche volume component are different: the precipitation variance and the correlation component are only correlated with the centroid latitude while the temperature variance and the EVI variance are correlated with both centroid latitude and range size (Table 2). The median ratio between Mahalanobis distance and determinant ratio is 2.43, suggesting that the distance between niche centroids is more important than niche volume differences in driving overall environmental niche dissimilarity among the 260 bird species. When the multiple regression on distance matrices (MRM) is applied, different components of the Bhattacharyya distance have different determining factors: the Mahalanobis distance is only correlated with centroid latitude while the determinant ratio is correlated with both range size and centroid latitude (Table 2).

3.3 | Comparison with other metrics

Community-level functional traits: The determinant of trait covariance matrix as the measure of functional diversity had the highest

FIGURE 3 Species-level environmental niche assessment. (a) Component-wise environmental niche volume differences and (b) Bhattacharyya distance of environmental niche between two example species (White-throated Swift, *Aeronautes saxatalis*; and Tricolored Blackbird, *Agelaius tricolor*) (c–f) Change of niche volume and pairwise niche dissimilarity among 260 bird species with range size and centroid latitude. Solid lines are the fitted linear regression. Shaded area represents 95% confidence interval of linear regression. See Table 2 for summary statistics

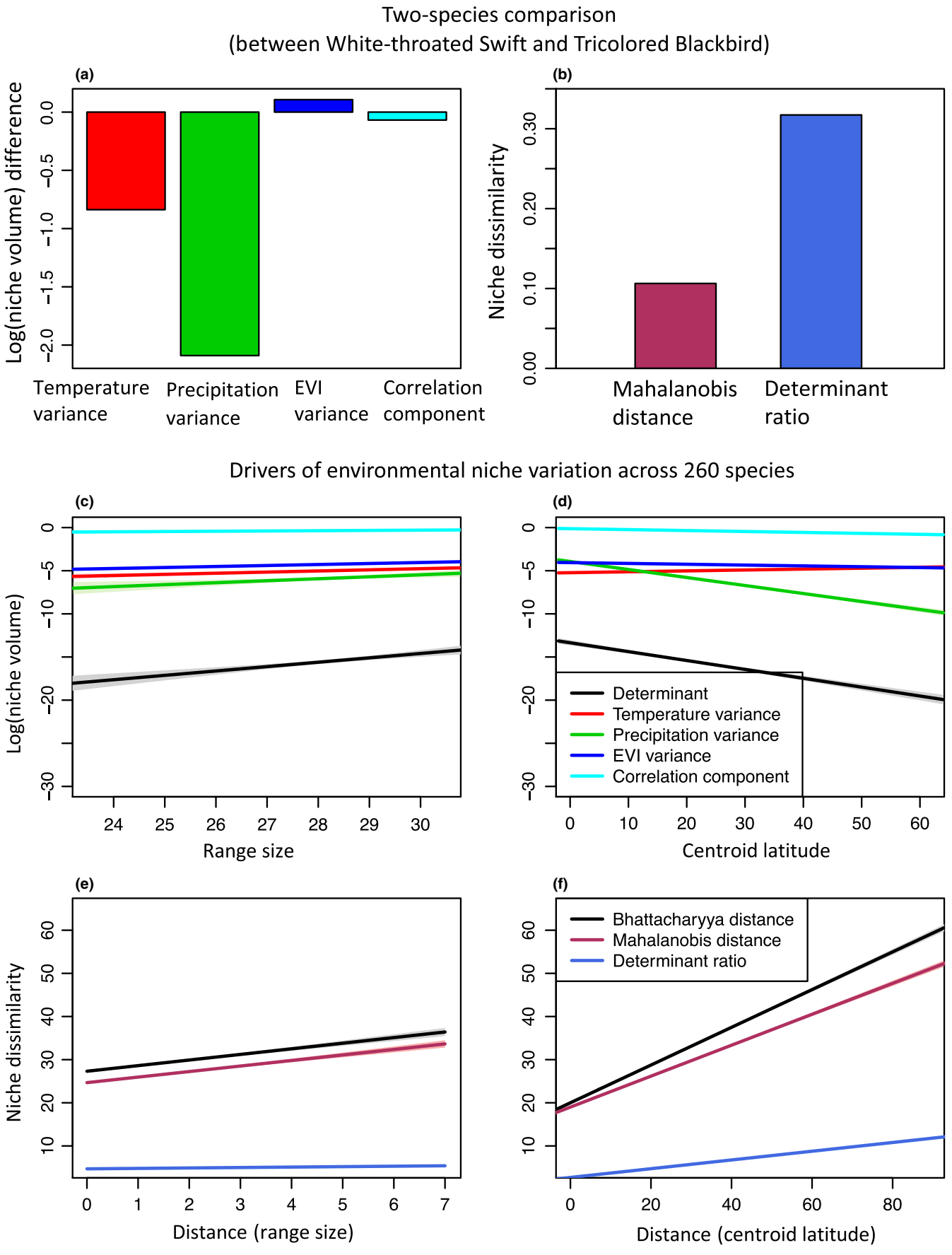
Two-species comparison
(between White-throated Swift and Tricolored Blackbird)
(a)
Log(niche volume) difference
0.0
−0.5
−1.0
−1.5
−2.0
Temperature variance
Precipitation variance
EVI variance
Correlation component
(b)
Niche dissimilarity
0.00
0.10
0.20
0.30
Mahalanobis distance
Determinant ratio
Drivers of environmental niche variation across 260 species
(c)
Log(niche volume)
0
−5
−10
−20
−30
24
25
26
27
28
29
30
Range size
(d)
0
−5
−10
−20
−30
Determinant
Temperature variance
Precipitation variance
EVI variance
Correlation component
0
10
20
30
40
50
60
Centroid latitude
(e)
Niche dissimilarity
10
20
30
40
50
60
0
1
2
3
4
5
6
7
Distance (range size)
(f)
Bhattacharyya distance
Mahalanobis distance
Determinant ratio
10
20
30
40
50
60
0
20
40
60
80
Distance (centroid latitude)

Response	Predictor	Estimate	*p*-value	R^2
Temperature variance	Area	1.13	<0.001	0.14
	Centroid latitude	0.84	<0.001	
Precipitation variance	Centroid latitude	−5.72	<0.001	0.69
EVI variance	Area	0.70	<0.001	0.13
	Centroid latitude	−0.46	<0.001	
Correlation component	Centroid latitude	−0.67	<0.001	0.22
Determinant	Area	2.09	<0.001	0.55
	Centroid latitude	−5.97	<0.001	
Mahalanobis distance	Distance (Centroid latitude)	32.62	<0.001	0.13
Determinant ratio	Distance (Area)	−2.66	<0.001	0.23
	Distance (Centroid latitude)	9.78	<0.001	
Bhattacharyya distance	Distance (Centroid latitude)	40.36	<0.001	0.15

TABLE 2 Summary statistics for multiple linear regression of environmental niche volumes, and multiple regression on distance matrices on environmental niche dissimilarity. Area, temperature, precipitation, EVI variances, the correlation component and the determinant are log-transformed. Adjusted R^2 is used. Only significant predictors are reported

correlation with the volume of the 95% quantile of a kernel-density-derived hypervolume (0.89), followed by functional dispersion (0.79) and minimum convex hull (0.65) (additional methods in Figure 4a). The Bhattacharyya distance had a similar correlation with Euclidean centroid distance (0.70), Jaccard similarity (−0.69) and Sorensen similarity (−0.71). The Mahalanobis distance component was more correlated with Euclidean centroid distance (0.73) than with Jaccard similarity (−0.57) or Sorensen similarity (−0.59) while the determinant ratio component had a relatively low correlation with the Euclidean centroid distance (0.42; Figure 4b). All components were uncorrelated with minimum distance between hypervolumes (Figure 4b).

Species-level environmental niche: the determinant of the environmental niche covariance matrix correlates most strongly with the volume of the 95% quantile of the kernel-density-derived hypervolume (0.85), followed by the minimum convex hull (0.77, Figure 4c). The Bhattacharyya distance and its Mahalanobis distance component are most correlated with the Euclidean centroid distance (0.85 and 0.82, respectively); the determinant ratio is similarly correlated with most alternative metrics except for minimum distance between hypervolumes (Figure 4d).

4 | DISCUSSION

We proposed a new parametric hypervolume framework based on multivariate normal distributions. The greatest advantage of the MVNH approach is the insights provided by the partitioned components of the niche size and dissimilarity metrics (Table 3). Although the determinant of the covariance matrix has been used as a total niche volume measure in some studies (La Sorte et al., 2018; Soberón & Nakamura, 2009), it has never been illustrated that the determinant can be interpreted as the product of individual niche variances and a correlation component. The Bhattacharyya distance has been used as a measure of home range overlap in animal movements (Fieberg & Kochanny, 2005; Winner et al., 2018). We suggest that its use in trait or environmental space (Lu et al., 1989; Minami & Shimizu, 1999), and in particular the interpretation of the partitioned components, offers valuable biological insights. Specifically, the correlation component of the determinant is a measure of the dimensionality of functional traits (see other dimensionality measures in He et al., 2020). The Mahalanobis distance between hypervolume centroids can be interpreted as the standardized distance between optimal traits of two communities or between the optimal environmental conditions of two species under the assumptions that mean community traits represent the optimal traits under equilibrium (Blonder et al., 2015) and that niche centroid has the highest fitness for a species (Sagarin et al., 2006). The determinant ratio can be interpreted as the functional diversity difference between communities or as niche volume differences between species. The Bhattacharyya distance (BD) not only avoids choosing ad hoc algorithm parameters, but more importantly reconciles the limitations of two commonly used classes of dissimilarity metrics (overlap metrics and distance metrics; Mammola, 2019). The overlap metrics (Jaccard and Sorensen indices) are used to calculate how much hypervolume is shared between the two hypervolumes, which are more informative when two hypervolumes intersect with each other. On the contrary, the distance metrics (centroid distance or minimum distance) are more informative when the hypervolumes are disjunct (Mammola, 2019). When Jaccard or Sorensen indices become uninformative for disjunct hypervolumes, the BD incorporates the distance information through the Mahalanobis distance component; when the centroid distance metric becomes uninformative for two close and overlapping hypervolumes, the BD incorporates the shape information through the determinant ratio component.

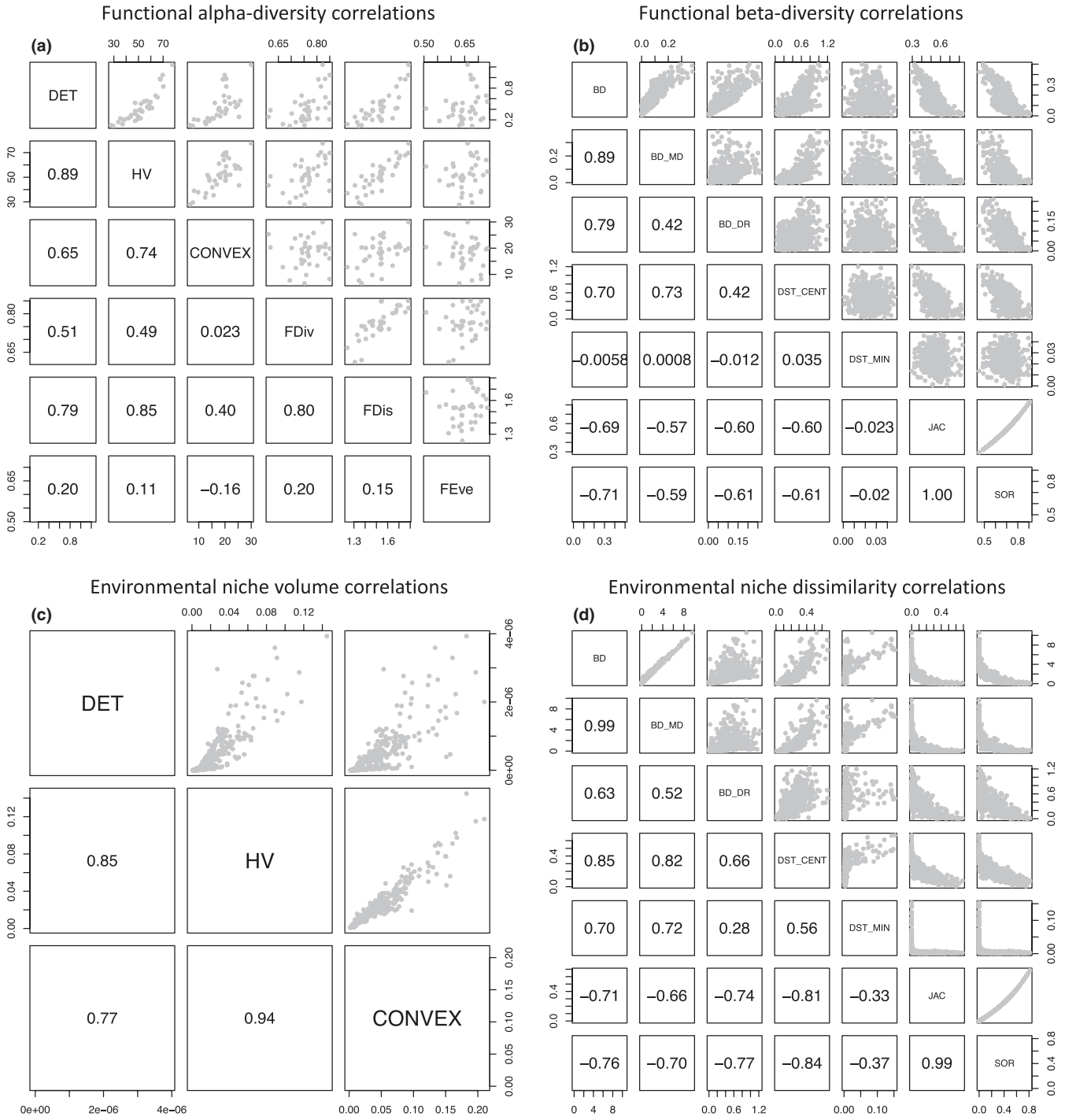

FIGURE 4 (a) Correlations among functional alpha diversity measures for the 36 sites. (b) Correlations among pairwise functional turnover measures. (c) Correlations among environmental niche volume measures for the 260 bird species. (d) Correlations among pairwise environmental niche dissimilarity measures. 'DET' stands for the determinant of the environmental niche or functional trait covariance matrix, 'HV' for kernel-density-derived hypervolume, 'CONVEX' for minimum convex hull, 'FDiv' for functional divergence, 'FDis' for functional dispersion, 'FEve' for functional evenness. 'BD' stands for Bhattacharyya distance, 'BD_MD' for the Mahalanobis distance component of BD, 'BD_DR' for the determinant ratio component of BD, 'DST_CENT' for Euclidean distance between centroids, 'DST_MIN' for minimum distance between kernel-density-derived hypervolumes, 'JAC' for Jaccard similarity, 'SOR' for Sorensen similarity

The good concordance between our method and the kernel density method in the empirical examples suggests that the determinant as a measure of niche volume is robust to different distributions of data. For niche dissimilarity measures, the moderate amount of correlation between the partitioned components of BD with the Jaccard, Sorensen and the centroid Euclidean distances shows that the partitioned components of BD both capture a part of the shape information of the hypervolume. Therefore, our BD

TABLE 3 Comparison of hypervolumes methods

	MVNH	Dynamic range box Junker et al. (2016)	nicheROVER Swanson et al. (2015)	Hypervolume Blonder et al. (2014)
(a) No assumptions about data distributions	✗	✓	✗	✓
(b) Allows holes in hypervolumes	✗	✗	✗	✓
(c) Does not require choosing a specific quantile	✓	✓	✗	✗[a]
(d) Sensitive to the number of dimensions[b]	✗	✗	✗	✓
(e) Provides information on the impact of individual dimensions to hypervolume variations	✓	✓	✗	✗
(f) Provides information on the impact of correlations among niche axes to hypervolume variations	✓	✗	✗	✗
(g) Partitions dissimilarity into size difference and turnover	✓[c]	✗	✗	✓[c]
(h) Dissimilarity metric incorporates distance information when hypervolumes do not overlap	✓	✗	✗	✗
(i) Computation time does not scale exponentially with the number of dimensions	✓	✓	✓	✗

[a]Hypervolume Blonder et al. (2014) additionally requires the choice of bandwidth for kernel density estimator.

[b]See Figure S4 in Appendix 1.

[c]The partitioning of the Hypervolume package is based on the framework of Baselga (2010) on overlap metrics. The counterpart of the turnover component in MVNH is the Mahalanobis distance component.

metrics combine the important interpretations of both centroid Euclidean distance metrics and the Jaccard and Sorensen metrics of niche dissimilarity. More importantly, the relative importance of centroid difference and volume difference are directly comparable using the BD metrics.

Other metrics such as the MacArthur–Levins measure (Equation 11), the Pianka's measure (Equation 12) and the Morisita's measure (Equation 13) can be similarly partitioned into a Mahalanobis distance component and a determinant ratio component (Lu et al., 1989), though their properties are less well known than the Bhattacharyya distance (Minami & Shimizu, 1999; Winner et al., 2018). We also show that the Mahalanobis distance component in all these metrics can be further partitioned into standardized Euclidean distances along different niche axes and a correlation component (Stevens, 1998), in addition to a previously proposed partitioning framework based on PCA (Calenge et al., 2008; Mahony et al., 2017).

4.1 | Case studies

Through the partitioning framework, our methods provide a novel understanding of each component driver of community functional diversity or species environmental niche volume. In the functional diversity example, we demonstrated that for the 36 annual plant communities the constraints on combination of traits is the major driver of functional alpha diversity which, in turn, is shaped by moisture availability; the major driver of functional community turnover is the variation of functional alpha diversity rather than the mean trait differences between communities. In the species environmental niche example, our method shows that the major driver of niche volume variation is the precipitation niche breadth variation (Figure 3d) which is determined by centroid latitude of species' range. We also show that the range size–niche breadth relationship of total environmental niche breadth is mainly driven by the range size–temperature niche breadth and range size–EVI niche breadth relationship (Table 2).

4.2 | Metrics performance

Simulation studies show that the bias of the plug-in estimator of the determinant is small with different sample sizes, distributions and number of dimensions (Figure S1). The plug-in estimator of the Bhattacharyya distance is slightly positively biased (Figures S2 and S3). The 95% confidence intervals of the Bhattacharyya distance components generally capture the theoretical values, except when the distance components are zero (Figure S2a,e). The biases are small compared to the estimated values, and small sample size leads to larger bias (Figures S2 and S3). Compared to the dynamic range box, nicheROVER and KDE methods, the Bhattacharyya distance has the smallest bias among other dissimilarity estimates and the bias is insensitive to the number of dimensions (Figure S4). Due to the parametric nature of our methods, the computational cost is significantly lower than other existing methods, especially for dissimilarity metrics with high-dimensional data (Figure S5). For example, using the 'Iris' dataset in R (a dataset with 150 rows and 3 columns), it takes 6 s to compute the hypervolume using KDE but only 0.001 s to compute the hypervolume using MVNH.

The biggest limitation of the MVNH framework is its assumption on normal distributions, which in many applications may not

be readily met, necessitating additional steps. Although we did not conduct a comprehensive analysis on how different distributions influence the volume and dissimilarity measures, we can gain insights about the effect of distributions through the lens of entropy. Entropy measures the dispersion of a distribution, which in the context of hypervolume can be viewed as a size measure in itself. For a multivariate normal distribution, the entropy is $\frac{1}{2}\ln det\ (2\pi e\Sigma)$, which is a monotonic transformation of the determinant of covariance matrix (the proposed size measure in the MVNH framework). It is also true that for all real-value distributions, that is, continuous distributions on $(-\infty, \infty)$, with a particular mean and variance, the normal distribution has the maximum entropy (Cover & Thomas, 2005). Therefore, the hypervolume size estimated by the MVNH framework could be interpreted as an upper bound on the hypervolume size across all other possible real-valued distributions. The influence on dissimilarity is less straightforward because it depends on two hypervolumes. Future research should extend the investigation to entropy (for both parametric and empirical distributions) as a hypervolume measure to fully understand the effect of different distributions on size and dissimilarity.

A common limitation of all hypervolume metrics is collinearity among axes (Blonder et al., 2014; D'Andrea & Ostling, 2016). The use of the determinant is especially sensitive to collinearity because any pair of fully dependent columns or rows in a covariance matrix will necessarily result in a determinant of zero. Increasing dimensions of trait or environmental data will increase the chance of collinearity and is also more likely to violate the multivariate normal assumption. Such an issue can be resolved by choosing the biologically relevant variables a priori or using common dimension reduction techniques applied in nonparametric methods such as PCA (Junker et al., 2016). Because PCA creates orthogonal axes, the correlation component will always equal 1 if PCA is applied, and thus it is only recommended when the correlation among axes is of no interest to the study. In the case of several groups of variables and relevant relationships among them (e.g. different sets of morphological traits of bird data; Pigot et al., 2020), more sophisticated dimension reduction techniques such as generalized canonical variables (Tenenhaus et al., 2014) can be used to select the most representative variables in each group. When the data are highly skewed, transformation to normal distribution is recommended.

4.3 | Potential

The presented size and dissimilarity measures are, to our knowledge, the first parametric metrics that allow a partitioning of n-dimensional hypervolumes. The partitioning of total niche volume and niche dissimilarity enables more rigorous testing of ecological and evolutionary hypotheses beyond those we explored in our two case studies. For example, when investigating the spatial scaling of niche volume (Connor et al., 2018; Pearman et al., 2008), the scaling relationship can be broken down to the scaling of univariate niche variances and correlation component, each of which can be linked to different sets of predictors. When studying niche shifts during biotic invasion (Hill et al., 2012; Lauzeral et al., 2011; Wiens et al., 2019), the BD can be used to determine whether the niche shift is mainly caused by shifts in niche centroids or caused by volume expansion or reduction, and which niche dimension contributes the most to different dissimilarity components. In niche evolution studies, the evolution of niche dissimilarity (Castro-Insua et al., 2018; Nunes & Pearson, 2017) between two species can be traced to contributions by niche breadth or centre differences to the total niche divergence. The parametric measures also have closer links to theory as theoretical predictions of niche evolution are usually derived from covariance matrices with multivariate normal approximations (Caetano & Harmon, 2019; Lande & Arnold, 1983). The framework can also be extended to include other aspects of functional diversity such as divergence and evenness (Mouchet et al., 2010; Villéger et al., 2008) by substituting the Euclidean distances between species with Mahalanobis distance in the calculations to fully incorporate intraspecific trait variations. The Euclidean distance is just a special case of the Mahalanobis distance by assuming that the intraspecific covariance matrix of functional traits is an identity matrix for all species within the community (unit variances and 0 correlations.). In other words, the newly proposed metrics have the potential to provide more mechanistic understanding of biodiversity patterns and niche evolution, and pave the way for more accurate forecasts for biodiversity change.

ACKNOWLEDGEMENTS

We thank Jetz Laboratory members for discussion of the work, especially Richard Li, Aurore Maureaud and Ben Carlson for comments on the first draft. We also thank Dr Stefano Mammola, Dr Robert Junker and an anonymous reviewer for their constructive and thoughtful comments. We acknowledge support from NSF grant DEB-1441737 and NASA grants 80NSSC17K0282 and 80NSSC18K0435.

CONFLICT OF INTEREST

The authors declare no conflict of interest.

AUTHORS' CONTRIBUTIONS

M.L. and W.J. conceived the ideas; M.L. analysed the data with substantial inputs from K.W. and W.J.; M.L. led the writing of the manuscript. All authors contributed critically to the drafts and gave final approval for publication.

PEER REVIEW

The peer review history for this article is available at https://publons.com/publon/10.1111/2041-210X.13665.

DATA AVAILABILITY STATEMENT

This paper contains no new data. Functions for calculating the size and dissimilarity metrics in the MVNH framework are available on GitHub in the package MVNH (Lu et al., 2021; https://github.com/lvmuyang/MVNH).

ORCID

Muyang Lu https://orcid.org/0000-0002-4949-8837
Kevin Winner https://orcid.org/0000-0002-8838-8905
Walter Jetz https://orcid.org/0000-0002-1971-7277

REFERENCES

Aiello-Lammens, M. E., Boria, R. A., Radosavljevic, A., Vilela, B., & Anderson, R. P. (2015). spThin: An R package for spatial thinning of species occurrence records for use in ecological niche models. *Ecography*, *38*(5), 541–545. https://doi.org/10.1111/ecog.01132

Baselga, A. (2010). Partitioning the turnover and nestedness components of beta diversity. *Global Ecology and Biogeography*, *19*(1), 134–143. https://doi.org/10.1111/j.1466-8238.2009.00490.x

Bhattacharyya, A. (1946). On a measure of divergence between two multinomial populations. *Bulletin of the Calcutta Mathematical Society*, *35*, 99–109.

Blonder, B. (2016). Do hypervolumes have holes? *The American Naturalist*, *187*(4), E93–E105. https://doi.org/10.1086/685444

Blonder, B. (2018). Hypervolume concepts in niche- and trait-based ecology. *Ecography*, *41*(9), 1441–1455. https://doi.org/10.1111/ecog.03187

Blonder, B., Lamanna, C., Violle, C., & Enquist, B. J. (2014). The n-dimensional hypervolume. *Global Ecology and Biogeography*, *23*(5), 595–609. https://doi.org/10.1111/geb.12146

Blonder, B., Morrow, C. B., Maitner, B., Harris, D. J., Lamanna, C., Violle, C., Enquist, B. J., & Kerkhoff, A. J. (2018). New approaches for delineating n-dimensional hypervolumes. *Methods in Ecology and Evolution*, *9*(2), 305–319. https://doi.org/10.1111/2041-210X.12865

Blonder, B., Nogués-Bravo, D., Borregaard, M. K., Donoghue, J. C., Jørgensen, P. M., Kraft, N. J. B., Lessard, J.-P., Morueta-Holme, N., Sandel, B., Svenning, J.-C., Violle, C., Rahbek, C., & Enquist, B. J. (2015). Linking environmental filtering and disequilibrium to biogeography with a community climate framework. *Ecology*, *96*(4), 972–985. https://doi.org/10.1890/14-0589.1

Brown, M. J. M., Holland, B. R., & Jordan, G. J. (2020). hyperoverlap: Detecting biological overlap in n-dimensional space. *Methods in Ecology and Evolution*, *11*(4), 513–523. https://doi.org/10.1111/2041-210X.13363

Caetano, D. S., & Harmon, L. J. (2019). Estimating correlated rates of trait evolution with uncertainty. *Systematic Biology*, *68*(3), 412–429. https://doi.org/10.1093/sysbio/syy067

Calenge, C., Darmon, G., Basille, M., Loison, A., & Jullien, J. M. (2008). The factorial decomposition of the Mahalanobis distances in habitat selection studies. *Ecology*, *89*(2), 555–566. https://doi.org/10.1890/06-1750.1

Cardillo, M., Dinnage, R., & McAlister, W. (2019). The relationship between environmental niche breadth and geographic range size across plant species. *Journal of Biogeography*, *46*(1), 97–109. https://doi.org/10.1111/jbi.13477

Carvalho, J. C., & Cardoso, P. (2020). Decomposing the causes for niche differentiation between species using hypervolumes. *Frontiers in Ecology and Evolution*. https://doi.org/10.3389/fevo.2020.00243

Castro-Insua, A., Gómez-Rodríguez, C., Wiens, J. J., & Baselga, A. (2018). Climatic niche divergence drives patterns of diversification and richness among mammal families. *Scientific Reports*, *8*(1), 8781. https://doi.org/10.1038/s41598-018-27068-y

Connor, T., Hull, V., Viña, A., Shortridge, A., Tang, Y., Zhang, J., Wang, F., & Liu, J. (2018). Effects of grain size and niche breadth on species distribution modeling. *Ecography*, *41*(8), 1270–1282. https://doi.org/10.1111/ecog.03416

Cover, T. M., & Thomas, J. A. (2005). *Elements of information theory*. https://doi.org/10.1002/047174882X

D'Andrea, R., & Ostling, A. (2016). Challenges in linking trait patterns to niche differentiation. *Oikos*, *125*(10), 1369–1385. https://doi.org/10.1111/oik.02979

Davies, S. J., Hill, M. P., McGeoch, M. A., & Clusella-Trullas, S. (2019). Niche shift and resource supplementation facilitate an amphibian range expansion. *Diversity and Distributions*, *25*(1), 154–165. https://doi.org/10.1111/ddi.12841

Díaz, S., Kattge, J., Cornelissen, J. H. C., Wright, I. J., Lavorel, S., Dray, S., Reu, B., Kleyer, M., Wirth, C., Colin Prentice, I., Garnier, E., Bönisch, G., Westoby, M., Poorter, H., Reich, P. B., Moles, A. T., Dickie, J., Gillison, A. N., Zanne, A. E., … Gorné, L. D. (2016). The global spectrum of plant form and function. *Nature*, *529*(7585), 167–171. https://doi.org/10.1038/nature16489

Dwyer, J. M., & Laughlin, D. C. (2017). Constraints on trait combinations explain climatic drivers of biodiversity: The importance of trait covariance in community assembly. *Ecology Letters*, *20*(7), 872–882. https://doi.org/10.1111/ele.12781

Dwyer, J. M., & Laughlin, D. C. (2018). Data from: Constraints on trait combinations explain climatic drivers of biodiversity: The importance of trait covariance in community assembly. *Dryad Digital Repository*, https://doi.org/10.5061/dryad.76kt8

Early, R., & Sax, D. F. (2014). Climatic niche shifts between species' native and naturalized ranges raise concern for ecological forecasts during invasions and climate change. *Global Ecology and Biogeography*, *23*(12), 1356–1365. https://doi.org/10.1111/geb.12208

Eckrich, C. A., Albeke, S. E., Flaherty, E. A., Bowyer, R. T., & Ben-David, M. (2020). rKIN: Kernel-based method for estimating isotopic niche size and overlap. *Journal of Animal Ecology*, *89*(3), 757–771. https://doi.org/10.1111/1365-2656.13159

Ficetola, G. F., Lunghi, E., & Manenti, R. (2020). Microhabitat analyses support relationships between niche breadth and range size when spatial autocorrelation is strong. *Ecography*, *43*(5), 724–734. https://doi.org/10.1111/ecog.04798

Fieberg, J., & Kochanny, C. O. (2005). Quantifying home-range overlap: The importance of the utilization distribution. *Journal of Wildlife Management*, *69*(4), 1346–1359. https://doi.org/10.2193/0022-541X(2005)69[1346:QHOTIO]2.0.CO;2

Gómez, C., Tenorio, E. A., Montoya, P., & Cadena, C. D. (2016). Niche-tracking migrants and niche-switching residents: Evolution of climatic niches in New World warblers (Parulidae). *Proceedings of the Royal Society B: Biological Sciences*, *283*(1824), 20152458. https://doi.org/10.1098/rspb.2015.2458

Gómez-Rodríguez, C., Baselga, A., & Wiens, J. J. (2015). Is diversification rate related to climatic niche width? *Global Ecology and Biogeography*, *24*(4), 383–395. https://doi.org/10.1111/geb.12229

González, A. L., Dézerald, O., Marquet, P. A., Romero, G. Q., & Srivastava, D. S. (2017). The multidimensional stoichiometric niche. *Frontiers in Ecology and Evolution*. https://doi.org/10.3389/fevo.2017.00110

Gruson, H. (2020). Estimation of colour volumes as concave hypervolumes using α-shapes. *Methods in Ecology and Evolution*, *11*(8), 955–963. https://doi.org/10.1111/2041-210X.13398

Guisan, A., Petitpierre, B., Broennimann, O., Daehler, C., & Kueffer, C. (2014). Unifying niche shift studies: Insights from biological invasions. *Trends in Ecology & Evolution*, *29*(5), 260–269. https://doi.org/10.1016/j.tree.2014.02.009

He, D., Biswas, S. R., Xu, M., Yang, T., You, W., & Yan, E. (2020). The importance of intraspecific trait variability in promoting functional niche dimensionality. *Ecography*, 1–11. https://doi.org/10.1111/ecog.05254

Hill, M. P., Hoffmann, A. A., Macfadyen, S., Umina, P. A., & Elith, J. (2012). Understanding niche shifts: Using current and historical data to model the invasive redlegged earth mite, Halotydeus destructor. *Diversity and Distributions*, *18*(2), 191–203. https://doi.org/10.1111/j.1472-4642.2011.00844.x

Holt, R. D. (2009). Bringing the Hutchinsonian niche into the 21st century: Ecological and evolutionary perspectives. *Proceedings of the National Academy of Sciences*, *106*(Supplement_2), 19659–19665. https://doi.org/10.1073/pnas.0905137106

Hutchinson, G. E. (1957). Concluding remarks. *Cold Spring Harbor Symposia on Quantitative Biology*, *22*, 415–427. https://doi.org/10.1101/SQB.1957.022.01.039

Jackson, A. L., Inger, R., Parnell, A. C., & Bearhop, S. (2011). Comparing isotopic niche widths among and within communities: SIBER - Stable Isotope Bayesian Ellipses in R. *Journal of Animal Ecology*, *80*(3), 595–602. https://doi.org/10.1111/j.1365-2656.2011.01806.x

Jiménez, L., Soberón, J., Christen, J. A., & Soto, D. (2019). On the problem of modeling a fundamental niche from occurrence data. *Ecological Modelling*, *397*(5), 74–83. https://doi.org/10.1016/j.ecolmodel.2019.01.020

Junker, R. R., Kuppler, J., Bathke, A. C., Schreyer, M. L., & Trutschnig, W. (2016). Dynamic range boxes – A robust nonparametric approach to quantify size and overlap of n-dimensional hypervolumes. *Methods in Ecology and Evolution*, *7*(12), 1503–1513. https://doi.org/10.1111/2041-210X.12611

Kuppler, J., Höfers, M. K., Trutschnig, W., Bathke, A. C., Eiben, J. A., Daehler, C. C., & Junker, R. R. (2017). Exotic flower visitors exploit large floral trait spaces resulting in asymmetric resource partitioning with native visitors. *Functional Ecology*, *31*(12), 2244–2254. https://doi.org/10.1111/1365-2435.12932

La Sorte, F. A., Fink, D., & Johnston, A. (2018). Seasonal associations with novel climates for North American migratory bird populations. *Ecology Letters*, *21*(6), 845–856. https://doi.org/10.1111/ele.12951

Laliberté, E., & Legendre, P. (2010). A distance-based framework for measuring functional diversity from multiple traits. *Ecology*, *91*(1), 299–305. https://doi.org/10.1890/08-2244.1

Lamanna, C., Blonder, B., Violle, C., Kraft, N. J. B., Sandel, B., imova, I., Donoghue, J. C., Svenning, J.-C., McGill, B. J., Boyle, B., Buzzard, V., Dolins, S., Jorgensen, P. M., Marcuse-Kubitza, A., Morueta-Holme, N., Peet, R. K., Piel, W. H., Regetz, J., Schildhauer, M., Spencer, N., Thiers, B., Wiser, S. K., & Enquist, B. J. (2014). Functional trait space and the latitudinal diversity gradient. *Proceedings of the National Academy of Sciences*, *111*(38), 13745–13750. https://doi.org/10.1073/pnas.1317722111

Lande, R., & Arnold, S. J. (1983). The measurement of selection on correlated characters. *Evolution*, *37*(6), 1210. https://doi.org/10.2307/2408842

Laughlin, D. C. (2014). The intrinsic dimensionality of plant traits and its relevance to community assembly. *Journal of Ecology*, *102*(1), 186–193. https://doi.org/10.1111/1365-2745.12187

Lauzeral, C., Leprieur, F., Beauchard, O., Duron, Q., Oberdorff, T., & Brosse, S. (2011). Identifying climatic niche shifts using coarse-grained occurrence data: A test with non-native freshwater fish. *Global Ecology and Biogeography*, *20*(3), 407–414. https://doi.org/10.1111/j.1466-8238.2010.00611.x

Leimar, O., Sasaki, A., Doebeli, M., & Dieckmann, U. (2013). Limiting similarity, species packing, and the shape of competition kernels. *Journal of Theoretical Biology*, *339*, 3–13. https://doi.org/10.1016/j.jtbi.2013.08.005

Lichstein, J. W. (2007). Multiple regression on distance matrices: A multivariate spatial analysis tool. *Plant Ecology*, *188*(2), 117–131. https://doi.org/10.1007/s11258-006-9126-3

Loiseau, N., Legras, G., Gaertner, J.-C., Verley, P., Chabanet, P., & Mérigot, B. (2017). Performance of partitioning functional beta-diversity indices: Influence of functional representation and partitioning methods. *Global Ecology and Biogeography*, *26*(6), 753–762. https://doi.org/10.1111/geb.12581

Lu, M., Winner, K., & Jetz, W. (2021). MVNH: An R package for calculating multivariate normal hypervolumes. *Zenodo*, https://doi.org/10.5281/zenodo.5006889

Lu, R.-P., Smith, E. P., & Good, I. J. (1989). Multivariate measures of similarity and niche overlap. *Theoretical Population Biology*, *35*(1), 1–21. https://doi.org/10.1016/0040-5809(89)90007-5

MacArthur, R., & Levins, R. (1967). The limiting similarity, convergence, and divergence of coexisting species. *The American Naturalist*, *101*(921), 377–385. https://doi.org/10.1086/282505

Mahony, C. R., Cannon, A. J., Wang, T., & Aitken, S. N. (2017). A closer look at novel climates: New methods and insights at continental to landscape scales. *Global Change Biology*, *23*(9), 3934–3955. https://doi.org/10.1111/gcb.13645

Mammola, S. (2019). Assessing similarity of n-dimensional hypervolumes: Which metric to use? *Journal of Biogeography*, *46*(9), 2012–2023. https://doi.org/10.1111/jbi.13618

Mammola, S., & Cardoso, P. (2020). Functional diversity metrics using kernel density n-dimensional hypervolumes. *Methods in Ecology and Evolution*, *11*(8), 986–995. https://doi.org/10.1111/2041-210X.13424

Minami, M., & Shimizu, K. (1999). Estimation of similarity measure for multivariate normal distributions. *Environmental and Ecological Statistics*, *6*(3), 229–248. https://doi.org/10.1023/A:1009678412953

Morisita, M. (1961). Measuring of interspecific association and similarity between communities. *Japanese Journal of Ecology*, *11*(6), 65–80. https://doi.org/10.18960/seitai.11.6_252_4

Mouchet, M. A., Villéger, S., Mason, N. W. H., & Mouillot, D. (2010). Functional diversity measures: An overview of their redundancy and their ability to discriminate community assembly rules. *Functional Ecology*, *24*(4), 867–876. https://doi.org/10.1111/j.1365-2435.2010.01695.x

Nunes, L. A., & Pearson, R. G. (2017). A null biogeographical test for assessing ecological niche evolution. *Journal of Biogeography*, *44*(6), 1331–1343. https://doi.org/10.1111/jbi.12910

Pearman, P. B., Guisan, A., Broennimann, O., & Randin, C. F. (2008). Niche dynamics in space and time. *Trends in Ecology & Evolution*, *23*(3), 149–158. https://doi.org/10.1016/j.tree.2007.11.005

Pianka, E. R. (1974). Niche overlap and diffuse competition. *Proceedings of the National Academy of Sciences*, *71*(5), 2141–2145. https://doi.org/10.1073/pnas.71.5.2141

Pigot, A. L., Sheard, C., Miller, E. T., Bregman, T. P., Freeman, B. G., Roll, U., Seddon, N., Trisos, C. H., Weeks, B. C., & Tobias, J. A. (2020). Macroevolutionary convergence connects morphological form to ecological function in birds. *Nature Ecology & Evolution*, *4*(2), 230–239. https://doi.org/10.1038/s41559-019-1070-4

Pigot, A. L., Trisos, C. H., & Tobias, J. A. (2016). Functional traits reveal the expansion and packing of ecological niche space underlying an elevational diversity gradient in passerine birds. *Proceedings of the Royal Society B: Biological Sciences*, *283*(1822), 20152013. https://doi.org/10.1098/rspb.2015.2013

Pironon, S., Villellas, J., Thuiller, W., Eckhart, V. M., Geber, M. A., Moeller, D. A., & García, M. B. (2018). The 'Hutchinsonian niche' as an assemblage of demographic niches: Implications for species geographic ranges. *Ecography*, *41*(7), 1103–1113. https://doi.org/10.1111/ecog.03414

Pulliam, H. R. (2000). On the relationship between niche and distribution. *Ecology Letters*, *3*(4), 349–361. https://doi.org/10.1046/j.1461-0248.2000.00143.x

Rappoldt, C., & Hogeweg, P. (1980). Niche packing and number of species. *The American Naturalist*, *116*(4), 480–492. https://doi.org/10.1086/283643

Read, Q. D., Grady, J. M., Zarnetske, P. L., Record, S., Baiser, B., Belmaker, J., Tuanmu, M.-N., Strecker, A., Beaudrot, L., & Thibault, K. M. (2018). Among-species overlap in rodent body size distributions predicts species richness along a temperature gradient. *Ecography*, *41*(10), 1718–1727. https://doi.org/10.1111/ecog.03641

Rolland, J., & Salamin, N. (2016). Niche width impacts vertebrate diversification. *Global Ecology and Biogeography*, *25*(10), 1252–1263. https://doi.org/10.1111/geb.12482

Sagarin, R. D., Gaines, S. D., & Gaylord, B. (2006). Moving beyond assumptions to understand abundance distributions across the ranges of species. *Trends in Ecology & Evolution*, *21*(9), 524–530. https://doi.org/10.1016/j.tree.2006.06.008

Saupe, E. E., Qiao, H., Hendricks, J. R., Portell, R. W., Hunter, S. J., Soberón, J., & Lieberman, B. S. (2015). Niche breadth and geographic range size as determinants of species survival on geological time scales. *Global Ecology and Biogeography*, *24*(10), 1159–1169. https://doi.org/10.1111/geb.12333

Serra-Varela, M. J., Grivet, D., Vincenot, L., Broennimann, O., Gonzalo-Jiménez, J., & Zimmermann, N. E. (2015). Does phylogeographical structure relate to climatic niche divergence? A test using maritime pine (*Pinus pinaster* Ait.). *Global Ecology and Biogeography*, *24*(11), 1302–1313. https://doi.org/10.1111/geb.12369

Slatyer, R. A., Hirst, M., & Sexton, J. P. (2013). Niche breadth predicts geographical range size: A general ecological pattern. *Ecology Letters*, *16*(8), 1104–1114. https://doi.org/10.1111/ele.12140

Soberón, J., & Nakamura, M. (2009). Niches and distributional areas: Concepts, methods, and assumptions. *Proceedings of the National Academy of Sciences*, *106*(Supplement_2), 19644–19650. https://doi.org/10.1073/pnas.0901637106

Stevens, G. V. G. (1998). On the inverse of the covariance matrix in portfolio analysis. *The Journal of Finance*, *53*(5), 1821–1827. https://doi.org/10.1111/0022-1082.00074

Sullivan, B. L., Wood, C. L., Iliff, M. J., Bonney, R. E., Fink, D., & Kelling, S. (2009). eBird: A citizen-based bird observation network in the biological sciences. *Biological Conservation*, *142*(10), 2282–2292. https://doi.org/10.1016/j.biocon.2009.05.006

Swanson, H. K., Lysy, M., Power, M., Stasko, A. D., Johnson, J. D., & Reist, J. D. (2015). A new probabilistic method for quantifying n-dimensional ecological niches and niche overlap. *Ecology*, *96*(2), 318–324. https://doi.org/10.1890/14-0235.1

Tayleur, C., Caplat, P., Massimino, D., Johnston, A., Jonzén, N., Smith, H. G., & Lindström, Å. (2015). Swedish birds are tracking temperature but not rainfall: Evidence from a decade of abundance changes. *Global Ecology and Biogeography*, *24*(7), 859–872. https://doi.org/10.1111/geb.12308

Tenenhaus, A., Philippe, C., Guillemot, V., Le Cao, K. A., Grill, J., & Frouin, V. (2014). Variable selection for generalized canonical correlation analysis. *Biostatistics*, *15*(3), 569–583. https://doi.org/10.1093/biostatistics/kxu001

Villéger, S., Mason, N. W. H., & Mouillot, D. (2008). New multidimensional functional diversity indices for a multifaceted framework in functional ecology. *Ecology*, *89*(8), 2290–2301. https://doi.org/10.1890/07-1206.1

Whittaker, R. H., Levin, S. A., & Root, R. B. (1973). Niche, habitat, and ecotope. *The American Naturalist*, *107*(955), 321–338. https://doi.org/10.1086/282837

Wiens, J. J., Litvinenko, Y., Harris, L., & Jezkova, T. (2019). Rapid niche shifts in introduced species can be a million times faster than changes among native species and ten times faster than climate change. *Journal of Biogeography*, *46*(9), 2115–2125. https://doi.org/10.1111/jbi.13649

Wilman, H., Belmaker, J., Simpson, J., de la Rosa, C., Rivadeneira, M. M., & Jetz, W. (2014). EltonTraits 1.0: Species-level foraging attributes of the world's birds and mammals. *Ecology*, *95*(7), 2027. https://doi.org/10.1890/13-1917.1

Winner, K., Noonan, M. J., Fleming, C. H., Olson, K. A., Mueller, T., Sheldon, D., & Calabrese, J. M. (2018). Statistical inference for home range overlap. *Methods in Ecology and Evolution*, *9*(7), 1679–1691. https://doi.org/10.1111/2041-210X.13027

Zurell, D., Gallien, L., Graham, C. H., & Zimmermann, N. E. (2018). Do long-distance migratory birds track their niche through seasons? *Journal of Biogeography*, *45*(7), 1459–1468. https://doi.org/10.1111/jbi.13351

SUPPORTING INFORMATION

Additional supporting information may be found online in the Supporting Information section.

How to cite this article: Lu, M., Winner, K., & Jetz, W. (2021). A unifying framework for quantifying and comparing n-dimensional hypervolumes. *Methods in Ecology and Evolution*, 00, 1–16. https://doi.org/10.1111/2041-210X.13665